WILEY-VCH

Supporting Information

Multifunctional Origami Patch for Minimally Invasive Tissue Sealing

Sarah J. Wu[#], Hyunwoo Yuk[#], Jingjing Wu, Christoph S. Nabzdyk, Xuanhe Zhao[*]*

S. J. Wu, Dr. H. Yuk, Dr. J. Wu, Prof. X. Zhao
Department of Mechanical Engineering, Massachusetts Institute of Technology, Cambridge, MA 02139, USA
*E-mail: hyunwoo@mit.edu (H.Y.), zhaox@mit.edu (X.Z.)

Prof. C. S. Nabzdyk
Department of Anesthesiology and Perioperative Medicine, Mayo Clinic, Rochester, MN 55905, USA

Prof. X. Zhao
Department of Civil and Environmental Engineering, Massachusetts Institute of Technology, Cambridge, MA 02139, USA

#These authors contributed equally to this work.

Supplementary Experimental Section

FTIR characterization: Chemical composition of the zwitterionic-interpenetrated elastomer layer was characterized by a transmission Fourier transform infrared spectroscope (FTIR 6700, Thermo Fisher) using a Germanium attenuated total reflectance (ATR) crystal (55 deg).

Microscope imaging: Scanning electron microscope (SEM) images of the patch were taken by using an SEM facility (JSM-6010LA, JEOL) with 5 nm gold sputtering to enhance image contrasts. Confocal microscope images were obtained by an upright confocal microscope (SP8, Leica) with 490 nm excitation wavelength for fluorescein and 570 nm excitation wavelength for Rhodamine Red™.

Preparation of the gelatin hydrogel tissue phantom: 10 w/w % gelatin (300 bloom) was dissolved in deionized water at 40 ℃. The gelatin solution was then poured on a glass mold with 5 mm spacers. The gelatin hydrogel tissue phantoms were prepared by cooling the poured solution at room temperature for 1 h.

Preparation of the pure zwitterionic hydrogel: 50 w/w % DMAPS, 0.5% w/w % Irgacure 2959, and 0.5% w/w % PEGDMA were dissolved in deionized water. The precursor solution was then poured on a glass mold with 1 mm spacers. The zwitterionic hydrogels were cured in a UV chamber (284 nm, 10 W power) for 60 min.

Quantification of blood entrapment: A sample of the multilayer patch (25.4 mm in width and 25.4 mm in length) was prepared and coated with silicone oil (100 cSt viscosity). The multilayer patch then placed onto a gelatin hydrogel tissue phantom submerged in blood with the hydrophobic oil

layer facing downward. The multilayer patch was pressed against the tissue phantom at varying applied pressures using a mechanical testing machine (2.5 kN load-cell, Zwick/Roell Z2.5) for 5 s. The blood entrapped at the adhered patch-tissue phantom interface was visualized by taking photographs. To quantify the blood-entrapped area, the photographs were processed and analyzed by using ImageJ.

Bacterial adhesion characterization: An engineered *Escherichia coli* (*E. coli*) strain that constitutively expresses green fluorescent protein (GFP) was prepared by following the previously reported protocol and cultured in Luria-Bertani broth (LB broth) overnight at 37 °C. 1 µL of bacteria culture diluted in 1 mL of fresh LB broth was placed on samples (1 cm × 1 cm) and incubated for 24 h at 37 °C.[31] After incubation, the samples were taken out and rinsed with phosphate buffered saline (PBS) to remove the free-floating bacteria, and imaged with a fluorescence microscope (Eclipse LV100ND, Nikon). The number of adhered *E. coli* on the samples per unit area (mm^2) were counted by Image J.

Fibrin deposition characterization: A 5 v/v % solution of fetal bovine serum (FBS) in PBS used to block the wells of a 24-well plate for 30 min. The wells were rinsed with PBS, then 6 mm-diameter samples were placed in the blocked wells. The samples were submerged in porcine blood spiked with Alexa Fluor® 488-labeled human fibrinogen conjugate (66 µg fibrinogen mL^{-1} blood, Thermo Fisher) and incubated on a shaker in 220 rpm at room temperature for 60 min. The samples were gently rinsed in PBS and fixed for 1 hr in 2.5 v/v% glutaraldehyde in 0.1 M phosphate buffer. The samples were then imaged with a fluorescence microscope (Eclipse LV100ND, Nikon) and analyzed by using ImageJ.

Mechanical characterization: Unless otherwise indicated, the multilayer patch was applied by applying 77.5 kPa pressure for 5 s by a mechanical testing machine or equivalent weight. Unless otherwise indicated, all mechanical tests on adhesion samples were performed 6 h after initial pressing to ensure equilibrium swelling of the adhered multilayer patch in wet environments. The application of commercially-available tissue adhesives followed the provided manual for each product. Unless otherwise indicated, all adhesion characterization was performed on patches adhered to blood-covered tissues.

To measure interfacial toughness, adhered samples with widths of 2.5 cm were prepared and tested by the standard 180-degree peel test (ASTM F2256) using a mechanical testing machine (2.5-kN load-cell, Zwick/Roell Z2.5). All tests were conducted with a constant peeling speed of 50 mm min^{-1}. The measured force reached a plateau as the peeling process entered the steady-state. Interfacial toughness was determined by dividing two times of the plateau force (for 180-degree peel test) with the width of the tissue sample (**Figure S12a**). Hydrophilic nylon filters (1 μm pore size, TISCH Scientific) were applied as a stiff backing for the multilayer patch. Poly(methyl methacrylate) (PMMA) films (with a thickness of 50 μm; Goodfellow) were applied using cyanoacrylate glue (Krazy Glue) as a stiff backing for the tissues.

To measure shear strength, the adhered samples with an adhesion area of 2.5 cm in width and 1 cm in length were prepared and tested by the standard lap-shear test (ASTM F2255) with a mechanical testing machine (2.5-kN load-cell, Zwick/Roell Z2.5). All tests were conducted with a constant tensile speed of 50 mm min^{-1}. Shear strength was determined by dividing the maximum force by the adhesion area (**Figure S12b**). Hydrophilic nylon filters were applied as a stiff backing for the multilayer patch. PMMA films were applied using cyanoacrylate glue (Krazy Glue) as a stiff backing for the tissues.

To measure tensile strength, the adhered samples with adhesion area of 2.5 cm in width and 2.5 cm in length were prepared and tested by the standard tensile test (ASTM F2258) with the mechanical testing machine. All tests were conducted with a constant tensile speed of 50 mm min^{-1}. Tensile strength was determined by dividing the maximum force with the adhesion area (**Figure S12c**). Aluminum fixtures were applied by using a cyanoacrylate glue to provide grips for the tensile tests.

The tensile properties and fracture toughness of the samples were measured using pure-shear tensile tests of thin rectangular samples (10 mm in length, 30 mm in width, and 0.5 mm in thickness) with a mechanical testing machine (20-N load-cell, Zwick/Roell Z2.5). All tests were conducted with a constant tensile speed of 50 mm min^{-1}. The fracture toughness of the samples was calculated based on tensile tests of unnotched and notched samples (**Figure S5**).

In vivo fibrous capsule characterization: All animal surgeries were reviewed and approved by the Committee on Animal Care at the Massachusetts Institute of Technology. Female Sprague Dawley rats (225-250 g, Charles River Laboratories) were used for all *in vivo* studies. Before implantation, the multilayer patch was prepared using aseptic techniques and was further sterilized for 3 h under UV light. For implantation in the dorsal subcutaneous space, rats were anesthetized using isoflurane (1–2% isoflurane in oxygen) in an anesthetizing chamber. Anesthesia was maintained using a nose cone. The back hair was removed and the animals were placed over a heating pad for the duration of the surgery. The subcutaneous space was accessed by a 1-2 cm skin incision per implant in the center of the animal's back. To create space for implant placement, blunt dissection was performed from the incision towards the animal shoulder blades. multilayer patches with hydrophobic polymer (PDMS) faces (n = 4), hydrophilic polymer (pristine hydrophilic PU) faces

(n = 4), and zwitterionic faces (n = 4) with the size of 10 mm in width and 20 mm in length were placed in the subcutaneous pocket created above the incision without detachment. The incision was closed using interrupted sutures (4-0 Vicryl, Ethicon) and 3-6 ml of saline were injected subcutaneously. Up to four implants were placed per animal ensuring no overlap between each subcutaneous pocket created. After 2 or 4 weeks following the implantation, the animals were euthanized by CO_2 inhalation. Subcutaneous regions of interest were excised and fixed in 10% formalin for 24 h for histological analyses.

Fixed tissue samples were placed into 70% ethanol and submitted for histological processing and H&E and Masson's Trichrome staining at the Hope Babette Tang (1983) Histology Facility in the Koch Institute for Integrative Cancer Research at the Massachusetts Institute of Technology. The thickness of fibrous capsule was measured under a bright-field digital microscope (Eclipse LV100ND, Nikon) based on histology slides of each sample. Representative histology images of each group were shown in the corresponding figures.

Ex vivo demonstrations: All *ex vivo* experiments were reviewed and approved by the Committee on Animal Care at the Massachusetts Institute of Technology. All porcine tissues and organs for *ex vivo* experiments (skin, trachea, aorta, esophagus, intestine) were purchased from a research-grade porcine tissue vendor (Sierra Medical Inc.). Heparinized porcine blood was purchased from Lampire Biological Laboratories, Inc. For sealing of a tracheal defect, a 5 mm-diameter hole was punched to a porcine trachea with a biopsy punch. The upper portion of the trachea was connected to a tubing, through which air was pumped to inflate the lung lobes. A multilayer patch was folded into an origami sleeve and introduced to a Foley catheter (ReliaMed). The Foley catheter with the multilayer patch was inserted into the lumen of the damaged trachea. Once the multilayer patch

was located below the defect, the balloon was inflated to apply pressure to the multilayer patch against the walls of the trachea for 5 s to seal the defect. After sealing of the tracheal defect, air was pumped through the trachea to check the air-tight sealing of the trachea and restored inflation capability of the lung lobes.

For sealing of an esophageal defect, a 5 mm-diameter hole was punched in the wall of a porcine esophagus with a biopsy punch. Water was flowed through the esophagus at 100 mmHg using a tubing and a peristaltic pump (Thermo Fisher) to visualize leakage through the defect. A multilayer patch was folded into an origami sleeve and introduced to an esophageal catheter (Boston Scientific). The esophageal catheter with the multilayer patch was inserted into the lumen of the damaged esophagus. Once the multilayer patch was located below the defect, the balloon was inflated to apply pressure to the multilayer patch against the walls of the esophagus for 5 s to seal the defect. After sealing of the esophageal defect, water was pumped through the trachea to check the fluid-tight sealing of the esophagus.

For sealing of an aortic defect, a 5 mm-diameter hole was punched in the wall of a porcine aorta with a biopsy punch. Porcine blood was flowed through the esophagus at 120 mmHg using a tubing and a peristaltic pump (Thermo Fischer) to visualize leakage through the defect. A multilayer patch was folded into an origami sleeve and introduced to a Foley catheter (ReliaMed). The Foley catheter with the multilayer patch was inserted into the lumen of the damaged aorta. Once the multilayer patch was located below the defect, the balloon was inflated to apply pressure to the multilayer patch and the walls of the aorta for 5 s to seal the defect. After sealing of the aortic defect, porcine blood was pumped through the aorta to check the fluid-tight sealing of the aorta.

For sealing of an intestinal defect, a 5 mm-diameter hole was punched to a porcine small intestine with a biopsy punch. A patch-loaded origami sleeve was folded and introduced to an articulating linear stapler (Ethicon). The articulating linear stapler with the multilayer patch was endoscopically navigated to the defect site and actuated to apply compression for 5 s. The repaired intestine was connected to a pump and inflated to check for fluid-tight sealing of the bowel. To simulate a minimally invasive surgical setting, the experiment was repeated inside a dark chamber with holes, and a waterproof endoscope camera (DEPSTECH) was used for visualization.

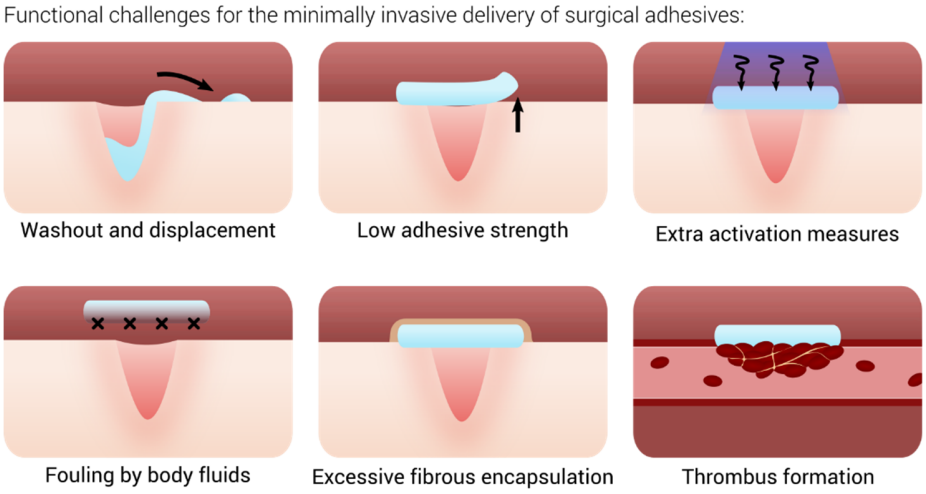

Figure S1. Functional limitations of existing bioadhesive materials for minimally invasive surgery.

Material & Form	Wet Tissue Adhesion	Body Fluid Resistance	Adhesion Speed	Adhesion Performance	Antifouling	MI Delivery & Application	Reference
Fibrin liquid glue	No	No	Slow (>3 min)	Low	No	Yes (injection)	FDA-approved product (Tisseel)
PEG liquid glue	No	No	Slow (>2 min)	Low	No	Yes (injection)	FDA-approved product (Coseal)
Cyanoacrylate liquid glue	No	No	Fast (<1 min)	High	No	N/R	FDA-approved product (Histoacryl)
Bulk tough hydrogel	Yes	Yes	Slow (>3 min)	High	No	No	*Science* **357**, 378 (2017)
Hydrophobic liquid glue	Yes	Yes	Slow (>2 min)	Intermediate	No	Yes (UV curing)	*Science Translational Medicine* **6**, 218ra6 (2014)
GelMA liquid glue	No	No	Slow (>2 min)	Intermediate	No	Yes (UV curing)	*Science Translational Medicine* **9**, eaai7466 (2017)
Double-sided tape	Yes	No	Fast (> 5 sec)	High	No	No	*Nature* **575**, 169-174 (2019)
Janus PACG & PACG-COS hydrogel patch	Yes	No	Fast (> 30 sec)	Intermediate	No	No	*Advanced Functional Materials*, 2005689 (2020)
Multilayer origami patch	Yes	Yes	Fast (>5 sec)	High	Yes	Yes	This work

* N/R: Not reported.

Supplementary Table 1. Comparison of various bioadhesives and their functional performance for minimally invasive surgery.

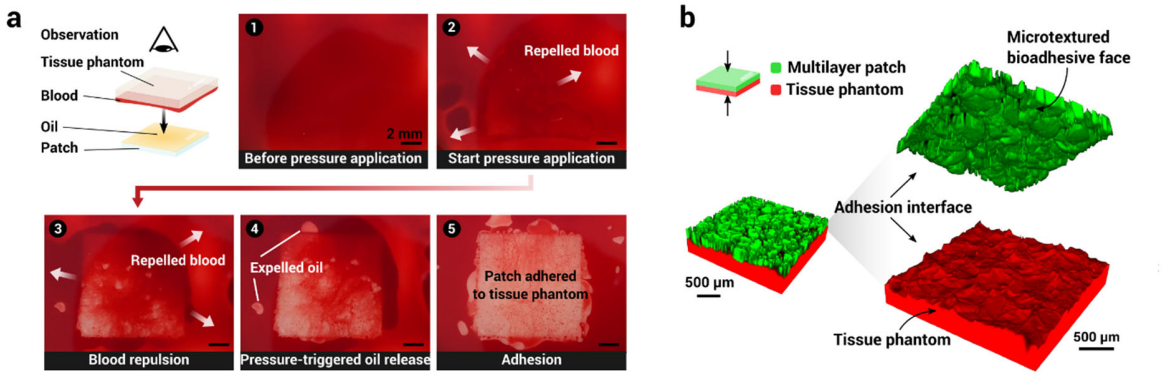

Figure S2. a) Photographs of the blood repellence and adhesion formation process between a multilayer patch and a gelatin hydrogel tissue phantom. b) 3D reconstruction of confocal micrographs at the interface of adhesion between the micro-textured bioadhesive face (green) and a tissue phantom of gelatin hydrogel (red).

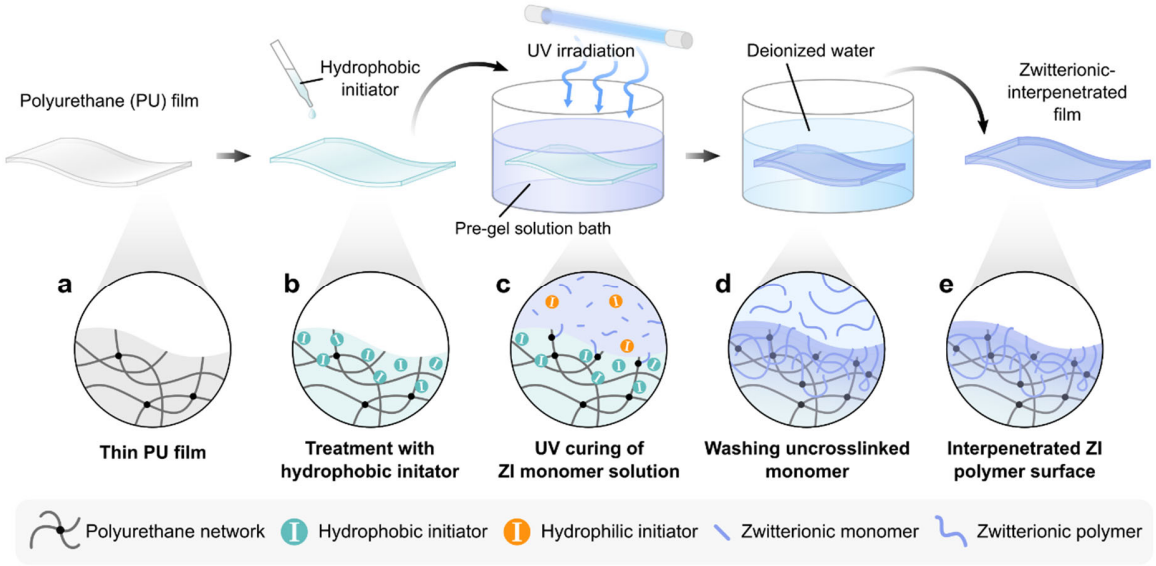

Figure S3. Preparation of the zwitterionic-interpenetrated elastomer antifouling layer. a-b) A thin film of hydrophilic PU is treated with a hydrophobic initiator (i.e., benzophenone). c) The treated hydrophilic PU film is submerged in a precursor solution containing the zwitterionic monomer and hydrophilic initiator (i.e., α-ketoglutaric acid), then cured in a UV chamber. d) The sample is washed in a large volume of deionized water. e) A zwitterionic-interpenetrated polyurethane film is retrieved.

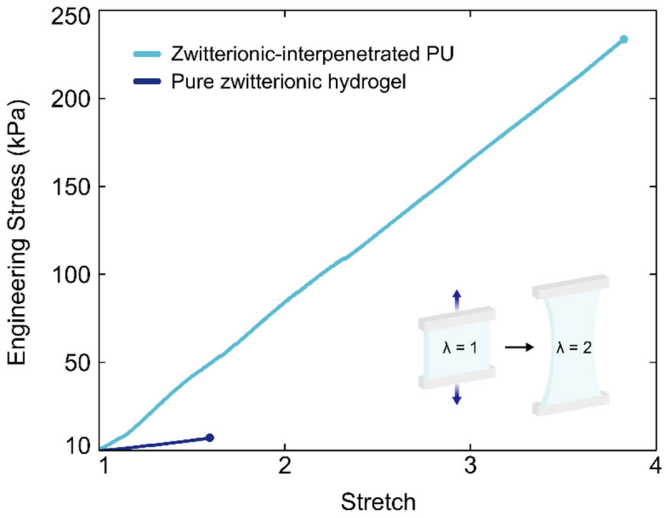

Figure S4. Representative engineering stress vs. stretch curves for the zwitterionic-interpenetrated polyurethane layer and a pure zwitterionic hydrogel.

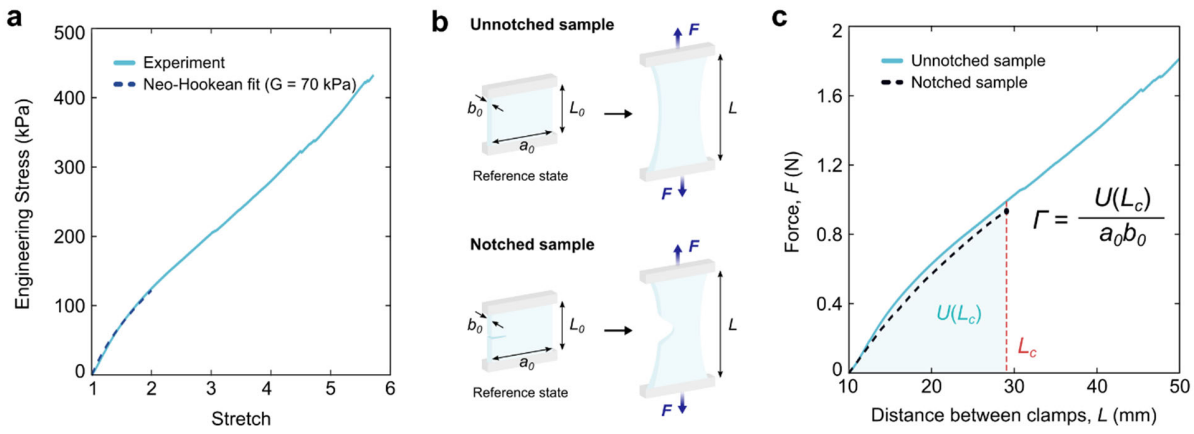

Figure S5. Mechanical characterization of the multilayer patch. a) Engineering stress vs. stretch curve of the multilayer patch. The measured shear modulus of the multilayer patch is 70 kPa. c) Schematic illustrations of a pure-shear test for unnotched and notched samples. c) Force vs. distance between clamps curves for the unnotched and notched antifouling face. L_c indicates the critical distance between the clamps at which the notch turns into a running crack. The measured fracture toughness of the multilayer patch is 2,100 J m^{-2}.

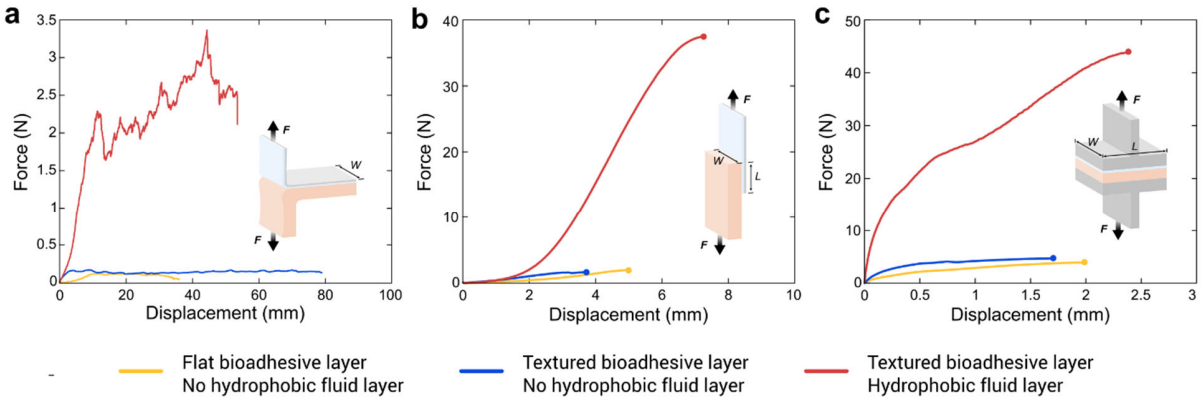

Figure S6. Representative force vs. displacement curves for a) 180-degree peel tests, b) lap-shear tests, and c) tensile tests of various multilayer patches adhered on blood-covered porcine skin. All patches were adhered to the tissue substrates by applying 77.5 kPa of pressure for 5 s.

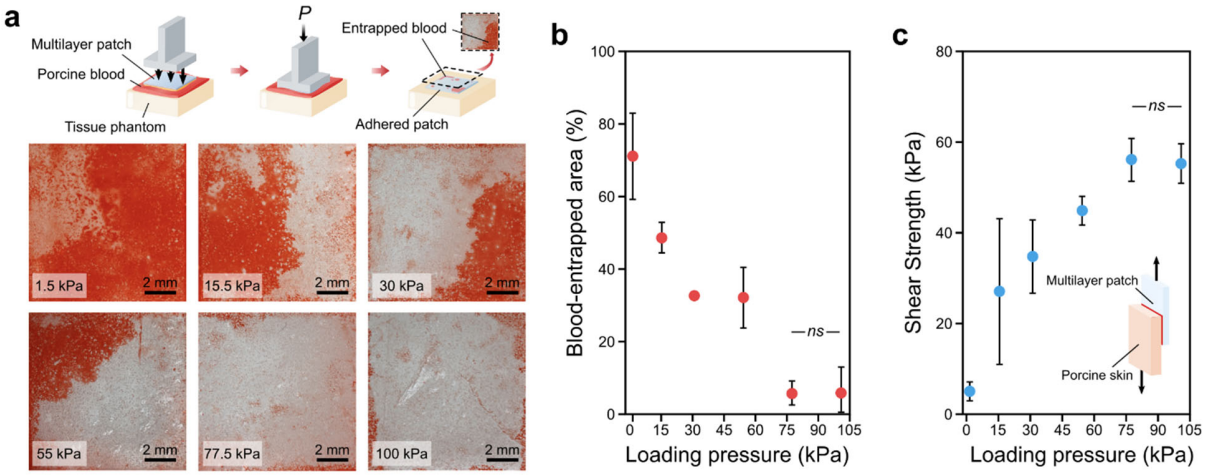

Figure S7. Characterization of blood repellence and adhesion performances of the multilayer patch under varying applied pressures. a) Representative photographs of the interfaces between the adhered multilayer patches and tissue phantom gelatin hydrogels. b) Percentage of blood-entrapped area at the interface as a function of applied pressure. c) Shear strength of adhered multilayer patches and blood-covered porcine skin as a function of applied pressure. Values in (b,c) represent the mean and the standard deviation ($n = 2$). *P* values are determined by a Student's t-test; * $p \leq 0.05$; ** $p \leq 0.01$; *** $p \leq 0.001$.

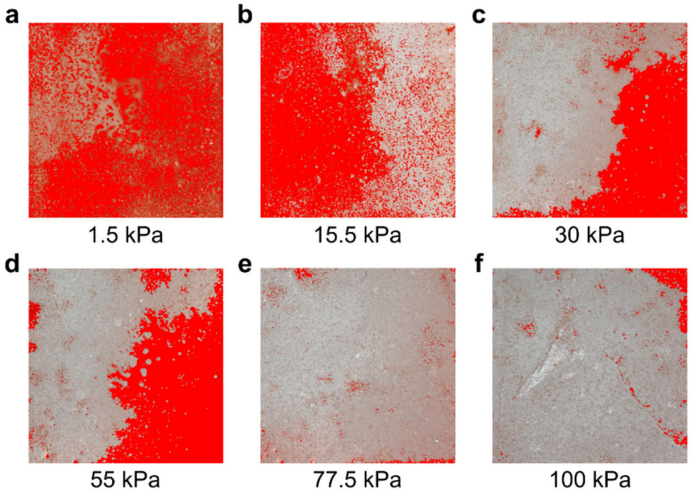

Figure S8. Representative processed images for the quantification of blood entrapment at the area of adhesion between the multilayer patches and blood-covered gelatin hydrogel tissue phantom compressed at 1.5 kPa (a), 15.5 kPa (b), 30 kPa (c), 55 kPa (d), 77.5 kPa (e), and 100 kPa (f) for 5 s. Photographs were processed by globally thresholding in ImageJ, then analyzed to quantify the percentage of blood-entrapped area.

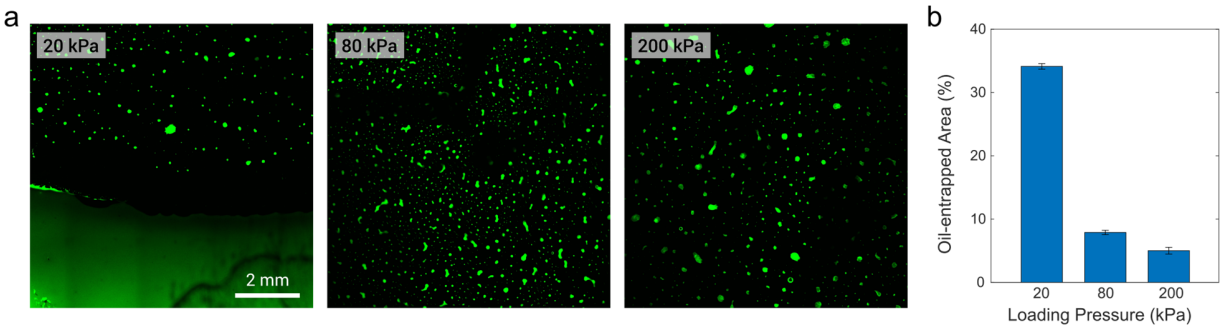

Figure S9. Interfacial oil entrapment as a function of applied pressure. a) Representative fluorescence micrographs of the adhesion interface between the bioadhesive patch and a gelatin tissue phantom substrate adhered under pressures of 20, 80, and 200 kPa. Residual fluorescently-dyed silicone oil can be visualized using fluorescent microscopy. b) Percentage of oil-entrapped area at the interface for loading pressures of 20, 80, and 200 kPa. The percentages of oil-entrapped area were 34.1 ± 0.4%, 7.9 ± 0.3%, and 5.0 ± 0.5%, respectively. Values represent the mean and standard deviation (n = 3).

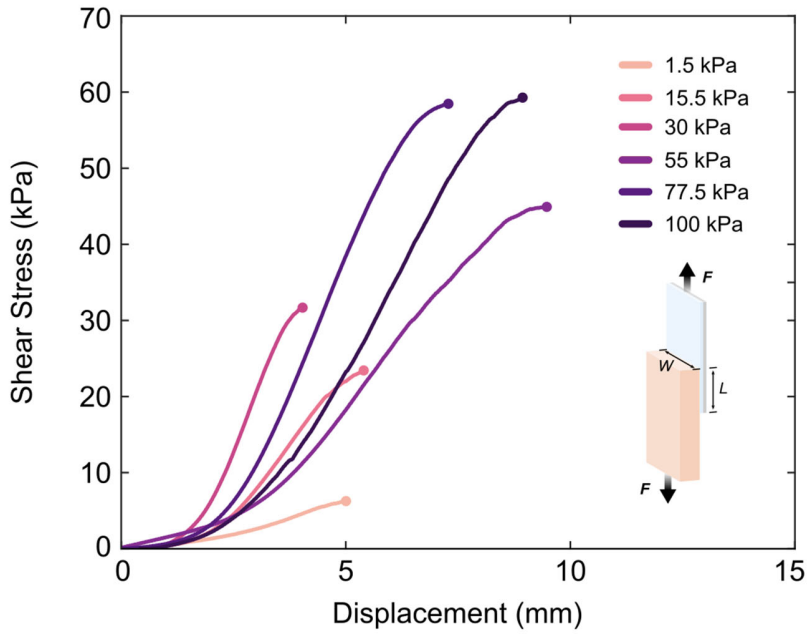

Figure S10. Shear stress vs. displacement curves for lap-shear tests of multilayer patches adhered to blood-covered porcine skins with varying applied pressures (1.5, 15.5, 30, 55, 77.5, and 100 kPa) for 5 s.

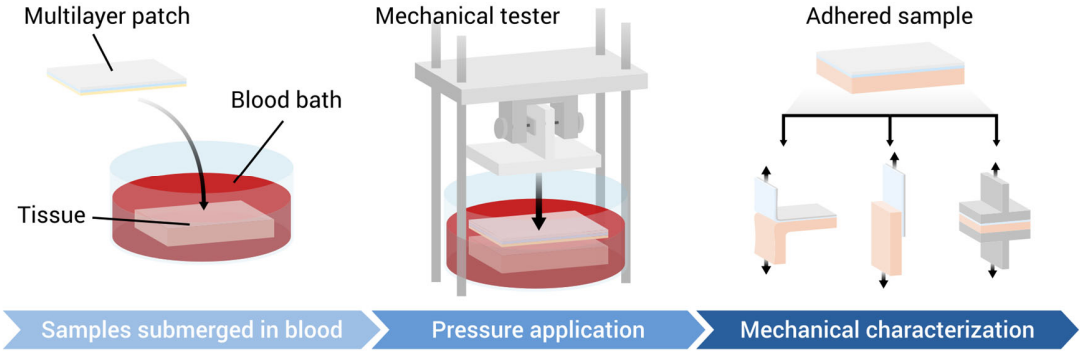

Figure S11. Experimental setup for the adhesion characterization of the multilayer patch and tissues submerged in blood. First, a sample of porcine tissue is covered with heparinized porcine blood. The multilayer patch is placed in the blood bath, then a mechanical tester applies a controlled pressure to adhere the patch to the tissue. After 5 s of pressure application, the adhered sample is collected for mechanical characterization to measure interfacial toughness, shear strength, or tensile strength, following ASTM standards F2256, F2255, and F2258.

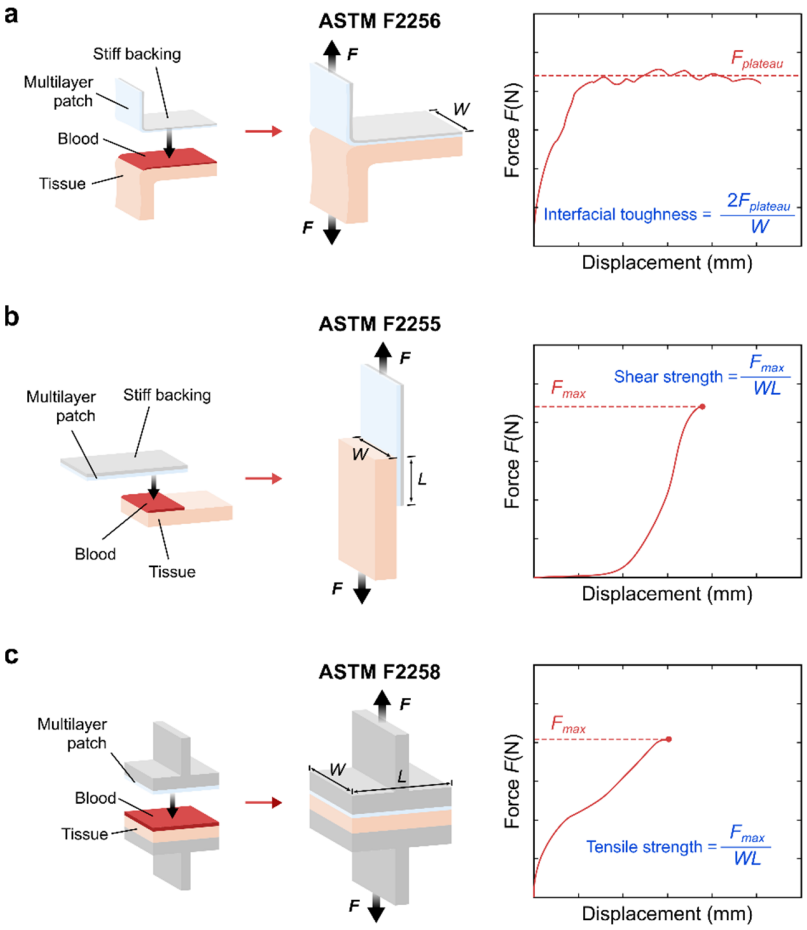

Figure S12. a) Schematic illustrations of the experimental setup for interfacial toughness measurements based on the standard 180-degree peel test (ASTM F2256). b) Schematic illustrations of the experimental setup for shear strength measurements based on the standard lap-shear test (ASTM F2255). c) Schematic illustrations of the experimental setup for tensile strength measurements based on the standard tensile test (ASTM F2258).

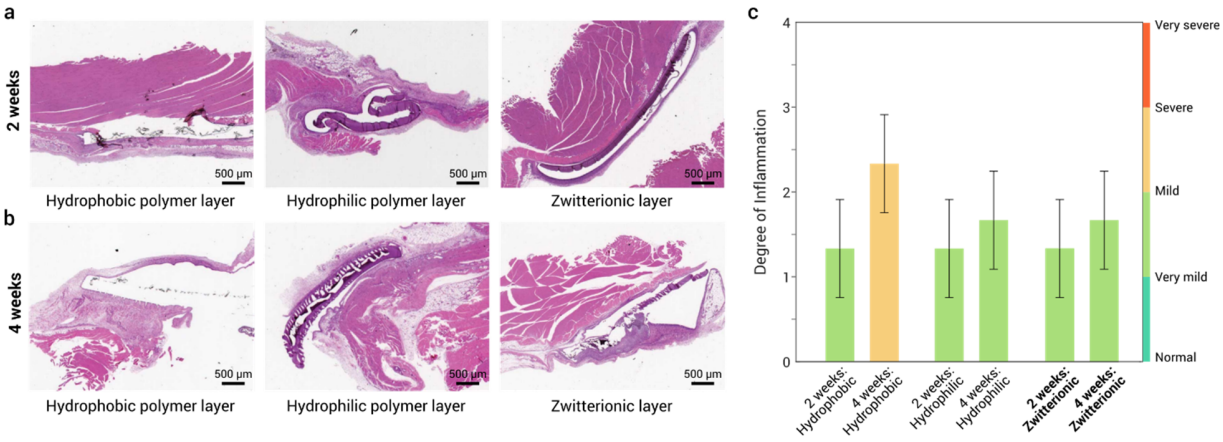

Figure S13. *In vivo* biocompatibility of the multilayer patch. Representative H&E histological images of multilayer patches with non-adhesive layers comprised of a hydrophobic polymer, a hydrophilic polymer, and a zwitterionic-interpenetrated elastomer layer implanted into the dorsal subcutaneous spaces of rats after a) 2 weeks and b) 4 weeks. c) Histological evaluation of the degree of inflammation at the implantation sites by a blinded pathologist. Degree of inflammation is scored wherein 0 = normal, 1 very mild, 2 = mild, 3 = severe, and 4 = very severe. Values represent the mean and standard deviation (n = 3).

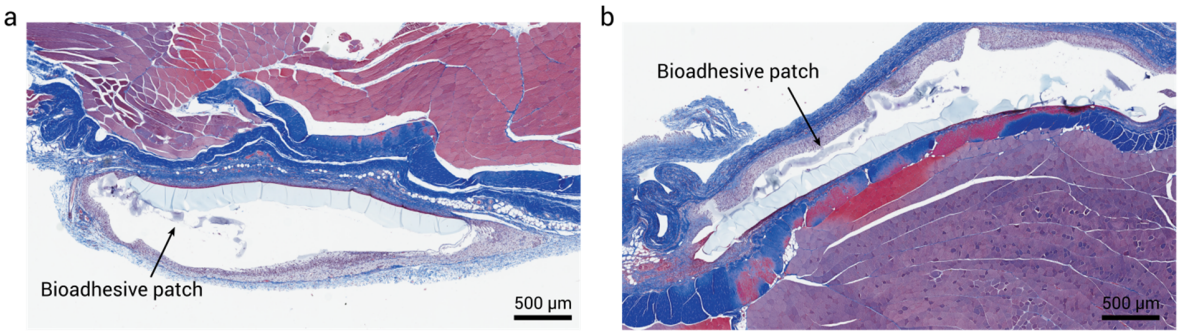

Figure S14. *In vivo* stability of the multilayer patch. Representative histological images stained with Masson's trichrome of samples implanted into the dorsal subcutaneous spaces of rats for a) 2 weeks and b) 4 weeks. At 4 weeks after implantation, the bioadhesive patch exhibits gradual degradation and decomposition.

Movie S1

Robust blood resistance of the multilayer patch against vigorous agitations in a porcine blood bath.

Movie S2

Minimally invasive delivery and sealing of an *ex vivo* porcine trachea by the multilayer patch.

Movie S3

Minimally invasive delivery and sealing of an *ex vivo* porcine esophagus by the multilayer patch.

Movie S4

Minimally invasive delivery and sealing of an *ex vivo* porcine aorta by the multilayer patch.

Movie S5

Minimally invasive delivery and sealing of an *ex vivo* porcine intestine by the multilayer patch.